

Strategy to Improve Photovoltaic Performance of DSSC Sensitized by Zinc Porphyrin Using Salicylic Acid as a Tridentate Anchoring Group

Faliang Gou,[†] Xu Jiang,[†] Ran Fang,[†] Huanwang Jing,^{*,†,‡} and Zhenping Zhu^{*,‡}

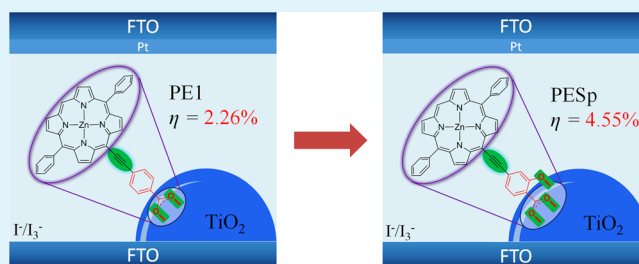
[†]State Key Laboratory of Applied Organic Chemistry, College of Chemistry and Chemical Engineering, Lanzhou University, Lanzhou 730000, China

[‡]State Key Laboratory of Coal Conversion, Institute of Coal Chemistry, Chinese Academy of Sciences, Taiyuan 030001, China

S Supporting Information

ABSTRACT: Three new zinc porphyrin dyes attached to ethynyl benzoic acid as an electron transmission and anchoring group have been designed, synthesized, and well-characterized. The performances of their sensitized solar cells have been investigated by optical, photovoltaic, and electrochemical methods. The photoelectric conversion efficiency of the solar cells sensitized by the dye with salicylic acid as an anchoring group demonstrated obvious enhancement when compared with that sensitized by the dye with carboxylic acid as an anchoring group. The density functional theory calculations and the electrochemical impedance spectroscopies revealed that tridentate binding modes could increase the efficiency of electron injection from dyes to the TiO₂ nanoparticles by more electron pathways.

KEYWORDS: dye-sensitized solar cell, anchoring group, salicylic acid, zinc porphyrin dye



INTRODUCTION

Growing global energy consumption, which has resulted in serious environmental issues, is impelling the requests and investigations about clean and renewable energy resources for development of a sustainable society. Solar energy, as a clean and continual energy sources, compared with traditional fossil fuel energy, provides a good choice for the development of such a society. Converting solar energy directly into electricity is the most feasible technology. Dye-sensitized solar cells (DSSCs),^{1–5} as a new generation of sustainable photovoltaic devices, have attracted extensive attention in view of their low cost, easy processing, and environmental benign property. It is well-known that photosensitizers play a key role in this type of DSSC, in which they catch photons and inject electrons into the conduction band of the TiO₂ semiconductor. Till now, the highest efficiencies of energy conversion have been achieved by the devices of DSSC using Ru polypyridyl complex^{6–8} and Zn porphyrin dyes^{9,10} as photosensitizers, respectively. Porphyrins have been the promising chromophores in terms of their virtual capture of solar energy in the region of visible light. Numerous zinc porphyrin dyes have been reported based on a donor- π spacer-acceptor (D- π -A) architecture, such as YD and LD series,^{11–14} which exhibited remarkably high efficiencies up to 12.3%.¹⁵

Generally, the standard anchoring group for sensitizers is carboxylic acid, which coordinates to the surface of TiO₂ nanoparticles by three binding modes.¹⁶ The efficient interfacial quantum yields of electron injection and collection from the dyes to the semiconductor surface intensely depend on anchoring groups and binding modes.^{17,18} Recently, we

mentioned that some groups focused on developing novel anchoring groups that would improve the photoelectric efficiency. For example, Yoon's group used the hydroxyl as an anchoring group in cat dyes;¹⁹ He's group applied 8-hydroxylquinoline as the anchoring group in metalloporphyrin sensitized solar cells;²⁰ Wang and Wu et al. introduced perylene anhydride into porphyrin dyes for this type of device;²¹ pyridine was also suggested as an anchoring group.^{22,23} Tian's group reported that 2-(1,1-dicyanomethylene) rhodanine is an alternative anchoring group for organic sensitizers.²⁴ Sun and his co-workers attempted the hydroxylpyridium connecting a dye to the surface of nano-TiO₂ that guarantees efficient electron-injection and regeneration.²⁵

In the quest for an efficient anchoring group for zinc porphyrin dyes and a successful strategy to enhance the photovoltaic performance and interfacial electron-transfer efficiency, we have reported that salicylic acid used as a tridentate anchoring group evidently augmented the interfacial quantum yields for azo-bridge zinc porphyrin in DSSCs.²⁶ To verify whether the polydentate binding modes of salicylic acids could improve the efficiency of charge injection and collection in other systems, we designed and synthesized three new zinc porphyrin dyes derived from the phenylethynylporphyrinato-zinc dye (PE1)^{27,28} and investigated their photovoltaic performance of DSSC to illustrate the importance of anchoring

Received: January 19, 2014

Accepted: April 24, 2014

Published: April 24, 2014

groups. The structures of zinc porphyrin dyes are shown in Figure 1.

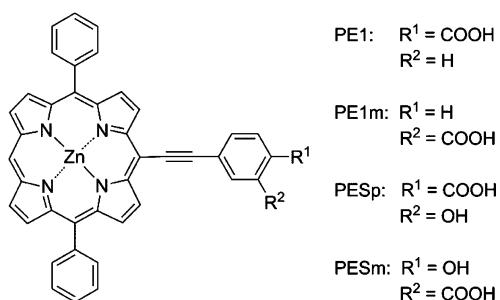


Figure 1. Structure of zinc porphyrin dyes.

EXPERIMENTAL SECTION

General. All solvents were treated by standard methods. All chemicals were of analytical grade and used as received. FTO glass was purchased from Nippon Sheet Glass Co. Ltd. (15 ohm/cm²). The NMR spectra were recorded on a Bruker AVANCE III 400 spectrometer using tetramethylsilane (TMS) as an internal standard. The MALDI-TOF mass spectra were acquired by a Bruker BIFLEX III spectrometer. The UV/vis absorption spectra were determined by an UV-3600 spectrophotometer in tetrahydrofuran (THF) at room temperature. The fluorescence spectra were obtained by an F-7000 fluorescence spectrophotometer.

Synthesis and Characterization of Dyes. General procedures for zinc porphyrin dyes are named as PE1, PE1m, PESp, and PESm. The synthetic protocols are shown in Figure 2. To a solution of [5,15-diphenyl-10-(triisopropylsilyl)ethynylporphinato] zinc(II) (0.1 mmol) in dry THF (10 mL) was added tetra-*n*-butylammonium fluoride (TBAF) (0.5 mL, 1 M in THF). The solution was stirred at 25 °C for 30 min under argon. The mixture was quenched with H₂O and then extracted with CH₂Cl₂. The combined organic layer was dried over anhydrous Na₂SO₄ for 2 h, and the solvent was removed under reduced pressure. The residue and iodobenzoic acid or iodosalicylic acid (0.5 mmol) were dissolved in a mixture of dry THF (25 mL) and

NEt₃ (4 mL) and then it was degassed. After Pd₂(dba)₃ (0.03 mmol) and AsPh₃ (0.2 mmol) were added to the mixture, the resulting solution was then refluxed for 12 h under argon. After the solution cooled down, the solvent was evaporated under reduced pressure. The crude product was purified by column chromatography (silica gel) using CH₂Cl₂/CH₃OH = 10/1 as eluent and recrystallized from CH₃OH/CH₂Cl₂ to yield pure zinc porphyrin dyes (40%–60%) as a green solid.

PE1. ¹H NMR (400 MHz; DMSO-*d*₆): δ 11.50 (1H, br, COOH), 10.33 (1H, s, meso-H), 9.84 (2H, d, *J* = 4.6 Hz, β-pyrrole), 9.44 (2H, d, *J* = 4.4 Hz, β-pyrrole), 8.92 (2H, d, *J* = 4.6 Hz, β-pyrrole), 8.84 (2H, d, *J* = 4.4 Hz, β-pyrrole), 8.22 (4H, m, Ar-H), 8.18 (4H, d, *J* = 2.5 Hz, Ar-H), 7.86 (6 H, m, Ar-H). ¹³C NMR (101 MHz; DMSO-*d*₆): δ 168.5, 151.5, 150.4, 149.7, 149.4, 142.6, 134.8, 133.1, 133.0, 132.3, 131.56, 131.0, 130.2, 128.2, 127.3, 126.9, 121.5, 108.8, 98.4, 95.8, 72.7, 60.7. MS (MALDI-TOF) calcd. for C₄₁H₂₄N₄O₂Zn: *m/z* 668.1. Found: 668.2 [M]⁺.

PE1m. ¹H NMR (400 MHz; DMSO-*d*₆): δ 11.95(1H, br, COOH), 10.33(1H, s, meso-H), 9.81 (2H, d, *J* = 4.5 Hz, β-pyrrole), 9.45 (2H, d, *J* = 4.5 Hz, β-pyrrole), 8.91 (2H, d, *J* = 4.5 Hz, β-pyrrole), 8.83 (2H, d, *J* = 4.5 Hz, β-pyrrole), 8.67 (1H, s, Ar-H), 8.21 (4H, m, Ar-H), 8.15 (1H, d, *J* = 7.5 Hz, Ar-H), 7.97 (1H, t, *J* = 7.5 Hz, Ar-H), 7.85 (6H, m, Ar-H), 7.78 (1H, d, *J* = 7.5 Hz, Ar-H). ¹³C NMR (101 MHz; DMSO-*d*₆): δ 170.8, 151.4, 150.3, 149.8, 149.4, 142.6, 134.8, 133.1, 132.9, 132.3, 131.0, 130.9, 129.4, 129.0, 128.9, 128.2, 128.1, 127.3, 121.3, 108.6, 98.8, 95.9, 94.7, 93.5. MS (MALDI-TOF) calcd. for C₄₁H₂₄N₄O₂Zn: *m/z* 668.1. Found: 668.2 [M]⁺.

PESp. ¹H NMR (400 MHz; DMSO-*d*₆): δ 14.15 (1H, br, OH), 11.58 (1H, br, COOH), 10.35 (1H, s, meso-H), 9.83 (2H, d, *J* = 4.6 Hz, β-pyrrole), 9.45 (2H, d, *J* = 4.5 Hz, β-pyrrole), 8.91 (2H, d, *J* = 4.6 Hz, β-pyrrole), 8.83 (2H, d, *J* = 4.5 Hz, β-pyrrole), 8.22 (4H, m, Ar-H), 8.03 (1H, d, *J* = 8.1 Hz, Ar-H), 7.86 (6H, m, Ar-H), 7.72 (1H, d, *J* = 1.5 Hz, Ar-H), 7.68 (1H, dd, *J* = 8.1, 1.5 Hz, Ar-H). ¹³C NMR (101 MHz; DMSO-*d*₆): δ 172.0, 161.7, 151.6, 150.5, 149.7, 149.4, 142.6, 134.8, 133.2, 133.1, 132.3, 131.4, 131.0, 130.7, 128.2, 127.3, 122.6, 121.6, 119.7, 113.6, 109.2, 97.7, 96.8, 95.2. MS (MALDI-TOF) calcd. for C₄₁H₂₄N₄O₃Zn: *m/z* 684.1. Found: 684.2 [M]⁺.

PESm. ¹H NMR (400 MHz; DMSO-*d*₆): δ 12.81 (1H, br, OH), 11.73 (1H, br, COOH), 10.25 (1H, s, meso-H), 9.78 (2H, d, *J* = 4.5 Hz, β-pyrrole), 9.41 (2H, d, *J* = 4.4 Hz, β-pyrrole), 8.89 (2H, d, *J* = 4.5 Hz, β-pyrrole), 8.82 (2H, d, *J* = 4.4 Hz, β-pyrrole), 8.37 (1H, d, *J* = 2.0

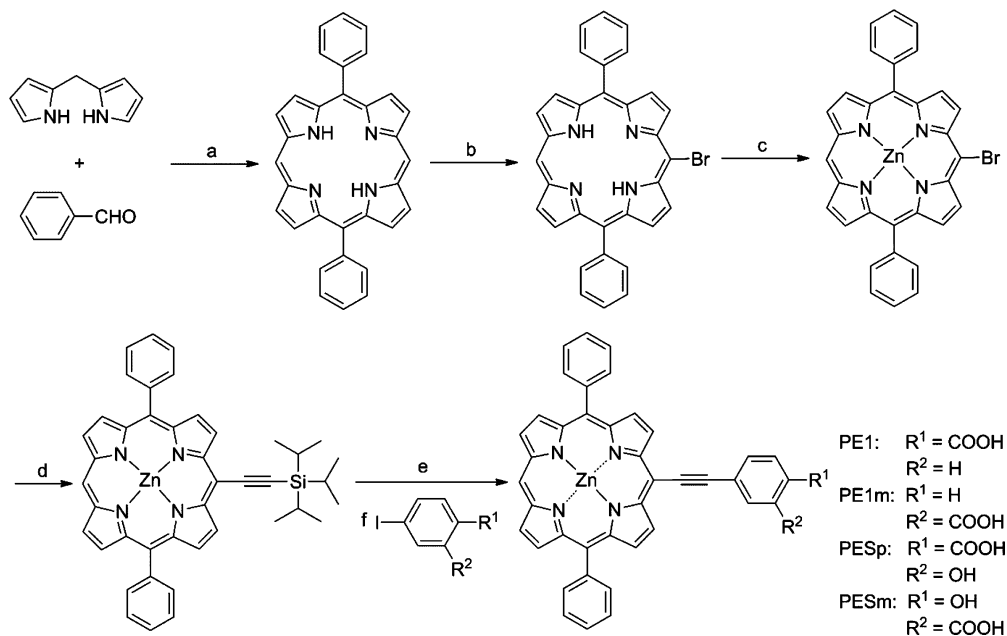


Figure 2. Synthetic protocol for zinc porphyrin dyes. (a) CF₃COOH; (b) NBS; (c) Zn(OAc)₂; (d) triisopropylacetylene, Pd(PPh₃)₂Cl₂, CuI, NEt₃; (e) TBAF; (f) Pd₂(dba)₃, AsPh₃, NEt₃.

Hz, Ar–H), 8.21 (4H, m, Ar–H), 7.94 (1H, dd, $J = 8.3, 2.0$ Hz, Ar–H), 7.85 (6H, m, Ar–H), 6.92 (1H, d, $J = 8.3$ Hz, Ar–H). ^{13}C NMR (101 MHz; DMSO- d_6): δ 171.2, 165.2, 151.2, 150.1, 149.9, 149.2, 142.8, 135.7, 134.8, 133.9, 132.8, 132.6, 132.3, 131.0, 128.1, 127.2, 121.1, 120.6, 117.8, 110.8, 107.8, 100.8, 97.6, 90.8. MS (MALDI-TOF) calcd. for $\text{C}_{41}\text{H}_{24}\text{N}_4\text{O}_3\text{Zn}$: m/z 684.1. Found: 684.2 $[\text{M}]^+$.

Photovoltaic Device Fabrication. The TiO_2 paste containing poly(ethylene glycol) and triton X-100 in a proportion of 33% weight was coated onto a commercial fluorine–tin-oxide (FTO) by vacuum spin-coater. The resulting TiO_2 film (thickness 15 μm and active area 0.16 cm^2) was then sintered at 450 $^\circ\text{C}$ for 1 h. When the system was cooled to 100 $^\circ\text{C}$, the photoanode was immersed immediately into the dye solution (0.5 mM, EtOH/toluene = 1/1, 2 h). The electrode was then taken out, washed with CH_3CN , and dried under argon. The solar cell was made by agglutinating the platinum counter electrode and the TiO_2 electrode. After the electrolyte containing 0.6 M DMPII, 0.05 M I_2 , and 0.5 M TBP in acetonitrile and valeronitrile (85:15, v/v) was primed to the TiO_2 film in vacuo, it was finally sealed by hot glue.

Photoelectrochemistry and Electrochemistry. The J – V curves were measured on a Keithley 2601A source meter with an AM-1.5 solar simulator (San-Ei XES-301S). The incident light intensity was 100 mW/cm^2 calibrated with an IEC 60904-3 standard Si solar cell (Fraunhofer ISE). The incident photon-to-current conversion efficiency (IPCE) of the cells was recorded by a Crown instrument, in which the tungsten halogen lamp (OSRAM HLX 64640 24 V 150W) was used as a light source using itself standard Si solar cell as a reference. The IPCE spectra can be calculated from the expression: $\text{IPCE}(\lambda) = (\text{sample current} \times \text{reference IPCE}(\lambda))/\text{reference current}$. Cyclic voltammetry trials were conducted using a CHI 660D instrument, with a traditional three-electrode system was assembled by glassy carbon electrode, a Ag/AgCl and Pt electrode. The electrochemical impedance spectroscopy (EIS) was achieved on a Zahner impedance analyzer (IM6ex) with Thales software. The amplitude of the AC signal was 10 mV and its frequency ranged between 0.1 and 1000,000 Hz. The data were plotted with Z-view software.

RESULTS AND DISCUSSION

Optical and Electrochemical Properties. The UV/vis spectra of the zinc porphyrin dyes are depicted in Figure 3. The maxima values and their molar absorption coefficients are shown in Table 1. The emission spectra of these dyes are illustrated in Figure 4 and their fluorescence data are also listed in Table 1. Owing to the similar structures, all the zinc porphyrin dyes exhibit the intense absorbing Soret bands (400–450 nm) and moderate absorbing Q bands (550–650 nm), which are attributed to the π – π^* electron transition. It was found that the dyes with salicylic acid group (PESp and PESm) showed little red shift in the maximum absorption wavelength (λ_{max}) and the maximum fluorescence emission wavelength (λ_{em}) than those of PE1 and PE1m with the carboxyl group. When these zinc porphyrin dyes were adsorbed onto the TiO_2 nanoparticle films, the adsorption spectra became broader and shifted toward longer wavelengths, which may be ascribed to the electronic coupling between porphyrin dyes and the TiO_2 semiconductor.²⁹ These phenomena indicated that the light-harvesting efficiency for these four zinc porphyrin dyes were very similar. The electrochemical properties of these porphyrins were investigated by cyclic voltammetry and presented in Table 1. Both porphyrin dyes showed the same E_{ox} values, which are more positive than the redox potential of I^-/I_3^- (0.4 V vs NHE) to ensure efficient regeneration.

Density Functional Theory (DFT) Calculations and Energy Levels. To understand the electronic structure of the dyes, their geometries and energies were fully optimized by

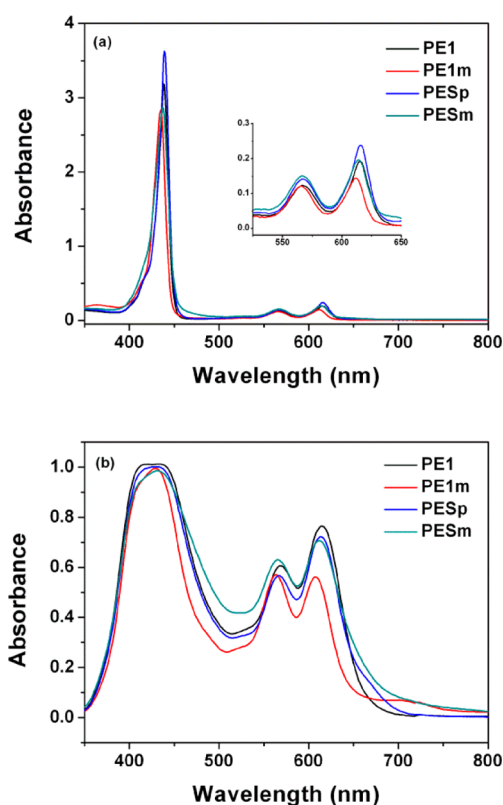


Figure 3. (a) UV/vis absorption spectra of zinc porphyrin dyes in THF. (b) UV/vis absorption spectra of zinc porphyrin dyes on TiO_2 film.

hybrid DFT using the standardized method of B3LYP/6-31G(d)/LANL2DZ.^{30,31} The molecular orbital diagrams of HOMO and LUMO are exhibited in Figure 5. The theoretical computed results elucidated that when the carboxyl group was located in the meta position of the ethyne bridge in PE1m as well as in PESm, the electrons in the frontier molecular orbital delocalized weakly from the zinc porphyrin core and ethyne bridge to the carboxyl group, which was unfavorable for electronic interaction between dye and the TiO_2 semiconductor; when the carboxyl group was located in the para position of ethyne bridge in the dyes of PE1 and PESp, the electrons in the frontier molecular orbital (LUMO) demonstrated higher efficient conjugation and strong electronic interaction between the extended π -conjugation and the anchoring group. The hydroxyl group also showed the electron density distribution at some level in PESp and PESm. It is clear that the electron density in the LUMO of PESp is more delocalized from metalloporphyrin center than that of PESm. Figure 6 shows the energy levels of zinc porphyrin dyes that were acquired by DFT calculations. The conducting band of TiO_2 is located between the LUMO and the HOMO of zinc porphyrin dyes. These results confirm that the propulsion of electron injection from LUMO to the conducting band is quite sufficient.

Photovoltaic Performance of DSSCs. The current density–voltage (J – V) curves of the devices with the zinc porphyrin dyes are shown in Figure 7 and the photovoltaic parameters were collected and are displayed in Table 2. The efficiencies of photoelectronic conversion of these cells demonstrated 2.26% (PE1), 0.64% (PE1m), 4.55% (PESp), and 1.22% (PESm), versus the reported efficiency 2.0% of

Table 1. Absorption/Emission and Electrochemical Properties of Zinc Porphyrin Dyes

dye	absorption ^a λ_{\max} (nm) (ϵ [$10^3 \text{ M}^{-1} \text{ cm}^{-1}$])	emission ^a λ_{em} (nm)	E_{0-0} ^b eV	E_{ox} ^c (V vs NHE)	$E_{\text{S}^+/\text{S}^*}$ ^d (V vs NHE)
PE1	438(319), 566(12.3), 615(19.2)	627, 677	2.10	1.01	-1.09
PE1m	435(284), 565(12.1), 612(14.4)	619, 671	2.11	1.02	-1.09
PESp	439(362), 567(14.2), 616(23.9)	628, 677	2.08	1.04	-1.04
PESm	437(286), 566(15.1), 614(19.7)	625, 677	2.08	1.00	-1.08

^aAbsorption and emission spectra were measured in THF solution at room temperature. ^b E_{0-0} was determined from the intersection of normalized absorption and emission spectra. ^cThe oxidation potentials of dyes were measured in THF with 0.1 M tetrabutylammonium hexafluorophosphate (TBAPF₆) with a scan rate of 50 mV s⁻¹ (vs NHE). ^d $E_{\text{S}^+/\text{S}^*}$ was calculated by $E_{\text{ox}} - E_{0-0}$.

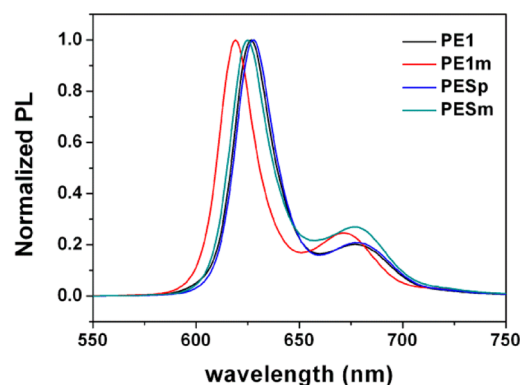


Figure 4. Normalized PL spectra of the porphyrin dyes in THF.

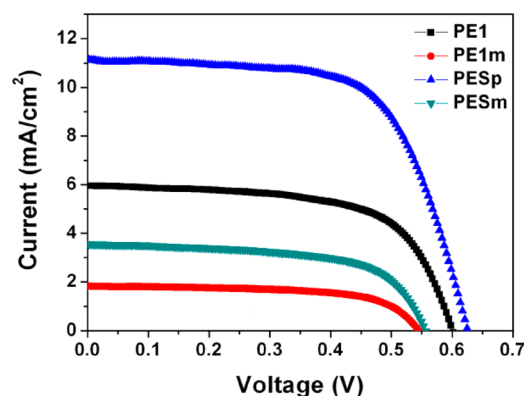
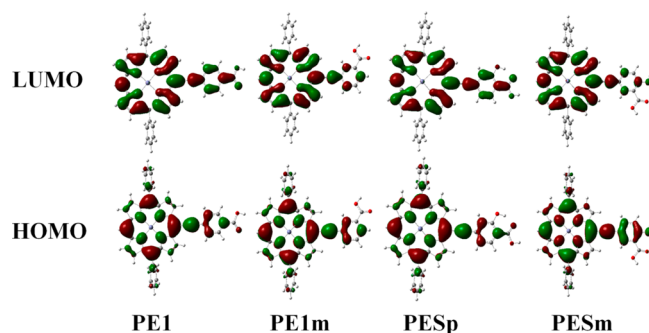
Figure 7. J - V characteristics of DSSCs sensitized by zinc porphyrin dyes.

Figure 5. Molecular orbitals of zinc porphyrin dyes.

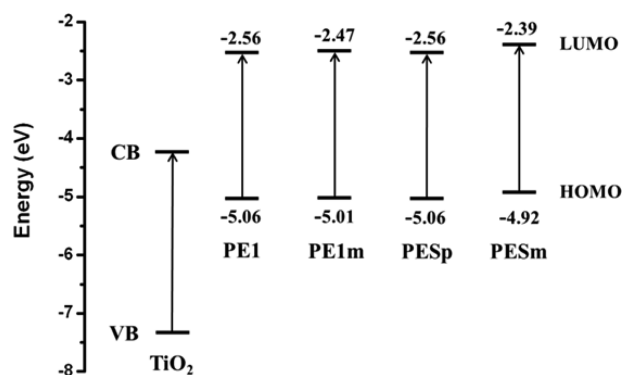


Figure 6. Energy-level diagram of zinc porphyrin dyes.

PE1.²⁸ In a comparison of PE1m with PE1, when the carboxylic group was moved to the meta position of the ethyne bridge, the short-circuit photocurrent density (J_{sc}) decreased from 5.95 to 1.83 mA/cm², and the open-circuit photovoltage (V_{oc}) also decreased from 0.60 to 0.55 V. These results revealed that the meta-carboxylic group was not conducive to charge injection. A similar phenomenon was observed in the cell performance

Table 2. Photovoltaic Performance of Dye Sensitized Solar Cells Based on Zinc Porphyrin Dyes

dye	V_{oc} (V)	J_{sc} (mA/cm ²)	FF (%)	η (%)
PE1	0.60	5.95	63.2	2.26
PE1m	0.55	1.83	63.7	0.64
PESp	0.63	11.14	64.9	4.55
PESm	0.56	3.55	61.9	1.22
N719	0.78	13.65	67.6	7.20

sensitized by PESm. Whereas, when the salicylic acid was used as the anchoring group in which the carboxylic group and hydroxyl group was located in the para and meta position of the ethyne bridge in PESp, the J_{sc} was promoted from 5.95 to 11.14 mA/cm² with the assistance of a hydroxyl group. Thus, the total photoelectronic conversion efficiency was enhanced up to 4.55%. The performance of these dyes with the salicylic acid as a tridentate anchoring group is superior than that with a carboxylic acid as the anchoring group.²⁶ On the other hand, the orientation of the carboxylic group and hydroxyl group also affects the photoelectric conversion efficiency due to the different transportation mode of electrons that can be clearly seen from the DFT calculation results.

The incident monochromatic photon-to-electron conversion efficiency (IPCE) spectra of the new dye-sensitized devices can be seen in Figure 8. The order of IPCE values of new dyes is as follows: PESp > PE1 > PESm > PE1m. The IPCE(λ) can be defined as $\text{IPCE}(\lambda) = \eta_{\text{LHE}}\eta_{\text{inj}}\eta_{\text{col}}$ (where η_{LHE} is the light harvesting efficiency, η_{inj} is the electron injection yield from the excited sensitizer into TiO₂, and η_{col} is the electron collection efficiency).^{2,15,32} The different IPCE values of four curves demonstrate that the salicylic acid, as a tridentate anchoring group, provides an efficient interfacial quantum yields of electron injection and collection from the metalloporphyrins to the semiconductor; also, the orientation of the carboxylic group is another important factor for this type of dye's designs. It is

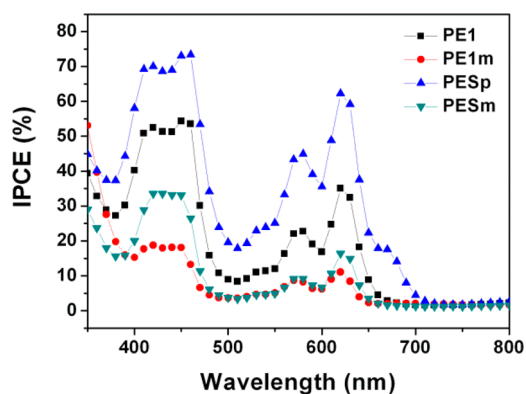


Figure 8. IPCE of DSSCs sensitized by zinc porphyrin dyes.

clearly seen from absorption spectra that the dyes have similar light-harvesting efficiencies (η_{LHE}), and the improvement of photoelectric conversion efficiency and IPCE was attributed to the electron injection (η_{inj}) and collection (η_{col}).

Electrochemical Impedance Spectroscopy. To further explain the enhancement of photovoltaic performance and IPCE of new dyes with salicylic acid as an efficient anchoring group, the interfacial charge transportation in the DSSC devices was investigated by electrochemical impedance spectroscopy, which was carried out at different applied potentials under dark conditions.^{33–36} The chemical capacitance (C_{μ}), the interfacial charge recombination resistance (R_{ct}), and the electron lifetime (τ_n) for PE1 and PESp are depicted in Figure 9, respectively. C_{μ} reflects quantitative information about the position of the conduction band.³⁷ The plots of C_{μ} value show that the positions of the conduction band edge of sensitized TiO_2 were similar. The electron recombination occurs at the interface between the semiconductor and the electrolyte, and this process always competes with the collection of electrons in the conduction band. In a comparison of the recombination resistance (R_{ct}) between two devices of PE1 and PESp, it can be seen that the value of R_{ct} for PESp is higher than that of PE1, indicating more difficult electron recombination. The larger the R_{ct} value, the more efficient the electron collection (η_{col}). The electron lifetime (τ_n) is plotted in Figure 9c as a function of bias potentials for PE1 and PESp, which is vitally important to the devices.^{38,39} The PESp device exhibited a relatively long electron lifetime compared with the PE1 device, because the salicylic acid binds to the interface, causing a delay of interaction between electrons and I_3^- ions, which benefit for the photovoltaic performance. Our results indicate that salicylic acids located in the para position of ethynyl as an anchoring group could facilitate the electron transportation from the dye to TiO_2 due to its intimate contact with the semiconductor surface via a tridentate binding mode by the carboxyl group and hydroxyl group, which furnishes more electron pathways.

CONCLUSION

In conclusion, the salicylic acid, as an anchoring group, has been introduced into the phenylethynyl porphyrinatozinc dyes. When the salicylic acids is located in the para position of ethynyl, a significant enhancement in photoelectric conversion efficiency of the zinc porphyrin dyes sensitized solar cells can be observed, which is double of that with only benzoic acid as the anchoring group by reason for a tridentate binding modes and a good orientation of functional groups between salicylic acid and TiO_2 nanoparticles, which should augment the interfacial

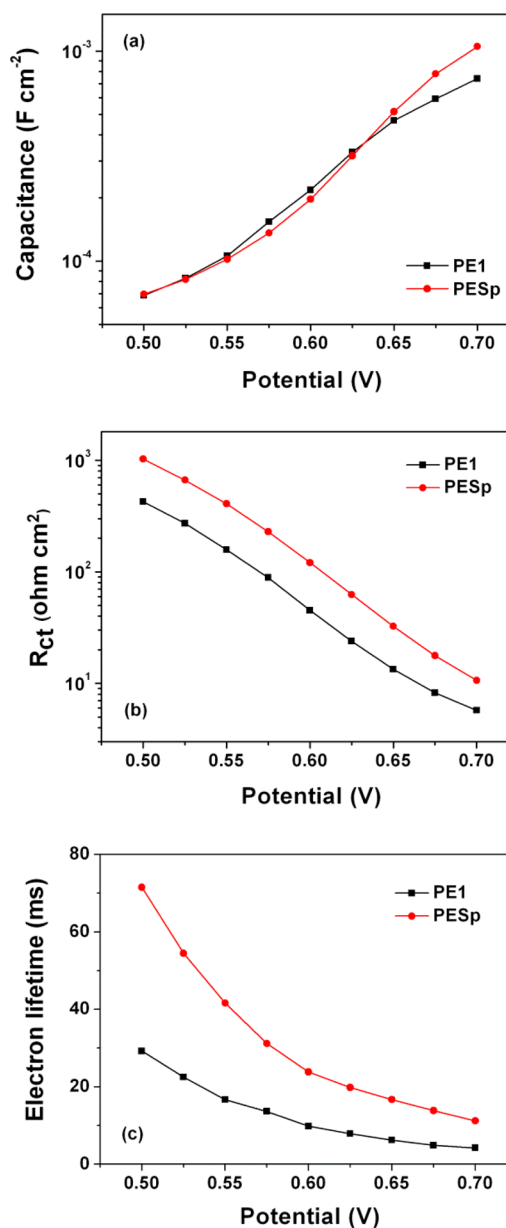


Figure 9. (a) Chemical capacitance, (b) the interfacial charge recombination resistance, and (c) the electron lifetime of zinc porphyrin dyes in DSSC. These data were obtained by fitting the impedance spectra of the devices measured in the dark under various biases.

quantum yields of electron injection and collection. This strategy should be increased in this field.

ASSOCIATED CONTENT

Supporting Information

Detailed synthetic routes, characteristic of the synthesized compounds, the dye-loading examination, and more calculation results. This material is available free of charge via the Internet at <http://pubs.acs.org>.

AUTHOR INFORMATION

Corresponding Authors

*H. Jing. E-mail: hwjing@lzu.edu.cn. Fax: 86-351-4048433. Tel: 86-931-8912585.

*Z. Zhu. E-mail: zpzhu@sxicc.ac.cn. Fax: 86-351-4048715. Tel: 86-931-8912585.

Notes

The authors declare no competing financial interest.

ACKNOWLEDGMENTS

The authors acknowledge the financial support of this work from the National Natural Science Foundation of China (NSFC 21173106) and by the Foundation of State Key Laboratory of Coal Conversion (Grant No. J14-15-913-1).

REFERENCES

- (1) O'Regan, B.; Grätzel, M. A Low-Cost, High-Efficiency Solar Cell Based on Dye-Sensitized Colloidal TiO₂ Films. *Nature* **1991**, *353*, 737–740.
- (2) Hagfeldt, A.; Boschloo, G.; Sun, L.; Kloo, L.; Pettersson, H. Dye-Sensitized Solar Cells. *Chem. Rev.* **2010**, *110*, 6595–6663.
- (3) Hardin, B. E.; Snaith, H. J.; McGehee, M. D. The Renaissance of Dye-Sensitized Solar Cells. *Nat. Photonics* **2012**, *6*, 162–169.
- (4) Ning, Z.; Fu, Y.; Tian, H. Improvement of Dye-Sensitized Solar Cells: What We Know and What We Need to Know. *Energy Environ. Sci.* **2010**, *3*, 1170–1181.
- (5) Zhang, S.; Yang, X.; Numata, Y.; Han, L. Highly Efficient Dye-Sensitized Solar Cells: Progress and Future Challenges. *Energy Environ. Sci.* **2013**, *6*, 1443–1464.
- (6) Nazeeruddin, M. K.; Kay, A.; Rodicio, I.; Humphry-Baker, R.; Mueller, E.; Liska, P.; Vlachopoulos, N.; Grätzel, M. Conversion of Light to Electricity by Cis-X₂bis(2,2'-Bipyridyl-4,4'-Dicarboxylate)-Ruthenium(II) Charge-Transfer Sensitizers (X = Cl⁻, Br⁻, I⁻, Cn⁻, and Scn⁻) on Nanocrystalline Titanium Dioxide Electrodes. *J. Am. Chem. Soc.* **1993**, *115*, 6382–6390.
- (7) Nazeeruddin, M. K.; De Angelis, F.; Fantacci, S.; Selloni, A.; Viscardi, G.; Liska, P.; Ito, S.; Takeru, B.; Grätzel, M. Combined Experimental and DFT-TDDFT Computational Study of Photoelectrochemical Cell Ruthenium Sensitizers. *J. Am. Chem. Soc.* **2005**, *127*, 16835–16847.
- (8) Yu, Q.; Wang, Y.; Yi, Z.; Zu, N.; Zhang, J.; Zhang, M.; Wang, P. High-Efficiency Dye-Sensitized Solar Cells: The Influence of Lithium Ions on Exciton Dissociation, Charge Recombination, and Surface States. *ACS Nano* **2010**, *4*, 6032–6038.
- (9) Li, L. L.; Diau, E. W. Porphyrin-Sensitized Solar Cells. *Chem. Soc. Rev.* **2013**, *42*, 291–304.
- (10) Campbell, W. M.; Burrell, A. K.; Officer, D. L.; Jolley, K. W. Porphyrins as Light Harvesters in the Dye-Sensitized TiO₂ Solar Cell. *Coord. Chem. Rev.* **2004**, *248*, 1363–1379.
- (11) Lee, C. W.; Lu, H. P.; Lan, C. M.; Huang, Y. L.; Liang, Y. R.; Yen, W. N.; Liu, Y. C.; Lin, Y. S.; Diau, E. W. G.; Yeh, C. Y. Novel Zinc Porphyrin Sensitizers for Dye-Sensitized Solar Cells: Synthesis and Spectral, Electrochemical, and Photovoltaic Properties. *Chem.—Eur. J.* **2009**, *15*, 1403–1412.
- (12) Chang, Y. C.; Wang, C. L.; Pan, T. Y.; Hong, S. H.; Lan, C. M.; Kuo, H. H.; Lo, C. F.; Hsu, H. Y.; Lin, C. Y.; Diau, E. W. G. A Strategy to Design Highly Efficient Porphyrin Sensitizers for Dye-Sensitized Solar Cells. *Chem. Commun.* **2011**, *47*, 8910–8912.
- (13) Ripolles-Sanchis, T.; Guo, B. C.; Wu, H. P.; Pan, T. Y.; Lee, H. W.; Raga, S. R.; Fabregat-Santiago, F.; Bisquert, J.; Yeh, C. Y.; Diau, E. W. G. Design and Characterization of Alkoxy-Wrapped Push-Pull Porphyrins for Dye-Sensitized Solar Cells. *Chem. Commun.* **2012**, *48*, 4368–4370.
- (14) Wang, C. L.; Lan, C. M.; Hong, S. H.; Wang, Y. F.; Pan, T. Y.; Chang, C. W.; Kuo, H. H.; Kuo, M. Y.; Diau, E. W. G.; Lin, C. Y. Enveloping Porphyrins for Efficient Dye-Sensitized Solar Cells. *Energy Environ. Sci.* **2012**, *5*, 6933–6940.
- (15) Yella, A.; Lee, H. W.; Tsao, H. N.; Yi, C.; Chandiran, A. K.; Nazeeruddin, M. K.; Diau, E. W. G.; Yeh, C. Y.; Zakeeruddin, S. M.; Grätzel, M. Porphyrin-Sensitized Solar Cells with Cobalt (II/III)–

Based Redox Electrolyte Exceed 12 Percent Efficiency. *Science* **2011**, *334*, 629–634.

(16) Galoppini, E. Linkers for Anchoring Sensitizers to Semiconductor Nanoparticles. *Coord. Chem. Rev.* **2004**, *248*, 1283–1297.

(17) O'Regan, B.; Xiaoe, L.; Ghaddar, T. Dye Adsorption, Desorption, and Distribution in Mesoporous TiO₂ Films, and Its Effects on Recombination Losses in Dye Sensitized Solar Cells. *Energy Environ. Sci.* **2012**, *5*, 7203–7215.

(18) Ooyama, Y.; Harima, Y. Photophysical and Electrochemical Properties, and Molecular Structures of Organic Dyes for Dye-Sensitized Solar Cells. *ChemPhysChem* **2012**, *13*, 4032–4080.

(19) Tae, E. L.; Lee, S. H.; Lee, J. K.; Yoo, S. S.; Kang, E. J.; Yoon, K. B. A Strategy to Increase the Efficiency of the Dye-Sensitized TiO₂ Solar Cells Operated by Photoexcitation of Dye-to-TiO₂ Charge-Transfer Bands. *J. Phys. Chem. B* **2005**, *109*, 22513–22522.

(20) He, H.; Gurung, A.; Si, L. 8-Hydroxyquinoline as a Strong Alternative Anchoring Group for Porphyrin-Sensitized Solar Cells. *Chem. Commun.* **2012**, *48*, 5910–5912.

(21) Jiao, C.; Zu, N.; Huang, K.-W.; Wang, P.; Wu, J. Perylene Anhydride Fused Porphyrins as near-Infrared Sensitizers for Dye-Sensitized Solar Cells. *Org. Lett.* **2011**, *13*, 3652–3655.

(22) Ooyama, Y.; Nagano, T.; Inoue, S.; Imae, I.; Komaguchi, K.; Ohshita, J.; Harima, Y. Dye-Sensitized Solar Cells Based on Donor-π-Acceptor Fluorescent Dyes with a Pyridine Ring as an Electron-Withdrawing-Injecting Anchoring Group. *Chem.—Eur. J.* **2011**, *17*, 14837–14843.

(23) Cui, J.; Lu, J.; Xu, X.; Cao, K.; Wang, Z.; Alemu, G.; Yuan, H.; Shen, Y.; Xu, J.; Cheng, Y.-B.; Wang, M. Organic Sensitizers with Pyridine Ring Anchoring Group for p-Type Dye-Sensitized Solar Cells. *J. Phys. Chem. C* **2014**, DOI: 10.1021/jp410829c.

(24) Mao, J.; He, N.; Ning, Z.; Zhang, Q.; Guo, F.; Chen, L.; Wu, W.; Hua, J.; Tian, H. Stable Dyes Containing Double Acceptors without Cooh as Anchors for Highly Efficient Dye-Sensitized Solar Cells. *Angew. Chem., Int. Ed.* **2012**, *51*, 9873–9876.

(25) Zhao, J.; Yang, X.; Cheng, M.; Li, S.; Sun, L. Molecular Design and Performance of Hydroxypyridium Sensitizers for Dye-Sensitized Solar Cells. *ACS Appl. Mater. Interfaces* **2013**, *5*, 5227–5231.

(26) Gou, F.; Jiang, X.; Li, B.; Jing, H.; Zhu, Z. Salicylic Acid as a Tridentate Anchoring Group for Azo-Bridged Zinc Porphyrin in Dye-Sensitized Solar Cells. *ACS Appl. Mater. Interfaces* **2013**, *5*, 12631–12637.

(27) Lin, C. Y.; Lo, C. F.; Luo, L.; Lu, H. P.; Hung, C. S.; Diau, E. W. G. Design and Characterization of Novel Porphyrins with Oligo-(Phenylethynyl) Links of Varied Length for Dye-Sensitized Solar Cells: Synthesis and Optical, Electrochemical, and Photovoltaic Investigation. *J. Phys. Chem. C* **2008**, *113*, 755–764.

(28) Luo, L.; Lin, C. J.; Tsai, C. Y.; Wu, H. P.; Li, L. L.; Lo, C. F.; Lin, C. Y.; Diau, E. W. G. Effects of Aggregation and Electron Injection on Photovoltaic Performance of Porphyrin-Based Solar Cells with Oligo(Phenylethynyl) Links inside TiO₂ and Al₂O₃ Nanotube Arrays. *Phys. Chem. Chem. Phys.* **2010**, *12*, 1064–1071.

(29) Seo, K. D.; Lee, M. J.; Song, H. M.; Kang, H. S.; Kim, H. K. Novel D-π-A System Based on Zinc Porphyrin Dyes for Dye-Sensitized Solar Cells: Synthesis, Electrochemical, and Photovoltaic Properties. *Dyes Pigm.* **2012**, *94*, 143–149.

(30) Rassolov, V. A.; Ratner, M. A.; Pople, J. A.; Redfern, P. C.; Curtiss, L. A. 6-31g* Basis Set for Third-Row Atoms. *J. Comput. Chem.* **2001**, *22*, 976–984.

(31) Hay, P. J.; Wadt, W. R. Ab Initio Effective Core Potentials for Molecular Calculations. Potentials for the Transition Metal Atoms Sc to Hg. *J. Chem. Phys.* **1985**, *82*, 270–283.

(32) Chen, J.; Li, B.; Zheng, J.; Jia, S.; Zhao, J.; Jing, H.; Zhu, Z. Role of One-Dimensional Ribbonlike Nanostructures in Dye-Sensitized TiO₂-Based Solar Cells. *J. Phys. Chem. C* **2011**, *115*, 7104–7113.

(33) Wang, Q.; Moser, J.-E.; Grätzel, M. Electrochemical Impedance Spectroscopic Analysis of Dye-Sensitized Solar Cells. *J. Phys. Chem. B* **2005**, *109*, 14945–14953.

(34) Fabregat-Santiago, F.; Garcia-Belmonte, G.; Mora-Sero, I.; Bisquert, J. Characterization of Nanostructured Hybrid and Organic

Solar Cells by Impedance Spectroscopy. *Phys. Chem. Chem. Phys.* **2011**, *13*, 9083–9118.

(35) Barea, E. M.; González-Pedro, V.; Ripollés-Sanchis, T.; Wu, H. P.; Li, L. L.; Yeh, C. Y.; Diao, E. W. G.; Bisquert, J. Porphyrin Dyes with High Injection and Low Recombination for Highly Efficient Mesoscopic Dye-Sensitized Solar Cells. *J. Phys. Chem. C* **2011**, *115*, 10898–10902.

(36) Fabregat-Santiago, F.; Bisquert, J.; Garcia-Belmonte, G.; Boschloo, G.; Hagfeldt, A. Influence of Electrolyte in Transport and Recombination in Dye-Sensitized Solar Cells Studied by Impedance Spectroscopy. *Sol. Energy Mater. Sol. Cells* **2005**, *87*, 117–131.

(37) Wang, M.; Chen, P.; Humphry-Baker, R.; Zakeeruddin, S. M.; Grätzel, M. The Influence of Charge Transport and Recombination on the Performance of Dye-Sensitized Solar Cells. *ChemPhysChem* **2009**, *10*, 290–299.

(38) Li, B.; Chen, J.; Zheng, J.; Zhao, J.; Zhu, Z.; Jing, H. Photovoltaic Performance Enhancement of Dye-Sensitized Solar Cells by Formation of Blocking Layers via Molecular Electrostatic Effect. *Electrochim. Acta* **2012**, *59*, 207–212.

(39) Zaban, A.; Greenshtein, M.; Bisquert, J. Determination of the Electron Lifetime in Nanocrystalline Dye Solar Cells by Open-Circuit Voltage Decay Measurements. *ChemPhysChem* **2003**, *4*, 859–864.